Evaluation of superalloy heavy-duty grinding based on multivariate tests

Q Liu, X Chen*, and **N Gindy**
School of Mechanical, Materials, and Manufacturing Engineering,
The University of Nottingham, Nottingham, UK

The manuscript was received on 22 December 2006 and was accepted after revision for publication on 17 May 2007.

DOI: 10.1243/09544054JEM809

Abstract: The quality and economy of grinding depend on proper selection of grinding conditions for the materials to be ground. In order to evaluate the effect of heavy-duty grinding, a new performance index, which includes specific material removal rate, size accuracy, and grinding forces, was proposed. Robust design of experiment, including orthogonal arrays, the signal-to-noise ratio (SNR) method, and analysis of variance (ANOVA) for multivariate data, was employed to estimate the effect of uniform experimental design and to optimize grinding parameters. Empirical models of grinding force were investigated for finite element analysis of new fixture design. These empirical models, based on robust design of experiments and multiple regression methodology, have been confirmed through further verification experiments. Correlation coefficients from 0.87 to 0.96 were achieved.

Keywords: grinding, robust design of experiment, empirical modelling

1 INTRODUCTION

The nickel-base alloy CMSX4 is used broadly in aerospace turbine engines, such as turbine blades and high pressure nozzle guide vanes (HP NGV) blades. This alloy consisting of elements with high melting point such as Ni, Cr, and Fe constructs an alloyed austenite of high purity and tightness with superlattices. Such an alloy has good hardness and strength at high temperatures. Grinding is one of the prime methods for this superalloy machining because of their property of being difficult-to-machine [**1**]. Modern manufacturing requires high efficiency, high precision, and low costs. The selection of grinding conditions, including grinding wheels, grinding parameters, and coolant delivery must achieve this goal. Grinding quality is described principally as surface roughness, surface integrity, size, and form accuracy [**2**]. Industry often demands that rough grinding conforms to required form and that finish grinding provides satisfactory surface integrity and accuracy [**3**, **4**]. Heavy-duty grinding is often used for rough grinding. The objective in heavy-duty grinding is rapid material removal with the desired workpiece size. The performance of heavy-duty grinding depends mainly on the material removal rate and wheel wear rate. A higher material removal rate means faster production, and a higher wheel-wear rate indicates increased wheel costs. Wheel consumption with conventional abrasives is usually a minor cost factor in precision grinding, but it can be very significant in heavy-duty grinding. There is generally a cost optimum material removal rate that balances higher wheel costs at faster material removal rates against lower stock removal costs. The material removal rate is always associated with grinding force through depth of cut [**5**].

Grinding force is a crucial issue in heavy-duty grinding. A large depth of cut and fast feed rate will cause a high grinding force. This can lead to many problems, such as size error, grinding chatter, and burn. If the wheel speed increases, grinding force and surface roughness will decrease. Therefore, high wheel speed should benefit grinding efficiency, but the wheel speed is limited by wheel structures and machine capability. Reduced grinding forces would expect components with small size error and superior surface integrity to be produced. In designing grinding fixture, it is vital to know the variation of grinding

**Corresponding author: School of Computing and Engineering, University of Huddersfield, Huddersfield HD1 3DH, UK. email: x.chen@hud.ac.uk*

force and the maximum grinding force. To do this, grinding force models are necessary in order to help improve the fixture structure based on finite element analysis.

From the manufacturing engineer's point of view, a model is the abstract representation of a process that serves to link causes and effects. Models can be subdivided into theoretical and empirical models. A theoretical model is derived deductively from basic physical principles, which help in the understanding of how grinding parameters influence the grinding performance. Empirical models are used in all fields of grinding technology owing to the fact that the physical interrelationship in grinding cannot be defined accurately. Normally, empirical models possess simple and easy-to-obtain characteristics but depend heavily on particular circumstances. Grinding performance can be related to an idealized chip shape and a different chip shape will lead to different grinding behaviour. Often, the grinding force model can be divided into a normal component and a tangential component respectively. In most cases grinding force is determined principally by the diameter of the grinding wheel d_e, the depth of cut a_e, the workpiece feed rate v_w, the spindle speed v_c, and the contact length l_g, etc. In general, if the wheel speed is increased, the grinding force and surface roughness decrease. Therefore, the high wheel speed should benefit grinding efficiency, but the wheel speed was limited by wheel structures and machine capability [**6**, **7**]. It should be pointed out that a coolant-induced force within the grinding process builds up in much the same way as the supporting force in hydrodynamic bearings. This force is often overlooked due to it being comparatively small. However, when coolant pressure reaches a certain level, it should no longer be ignored. The study showed that specific coolant-induced forces were between 4 and 6 N/mm when the spindle speed was lower than 60 m/s and specific coolant flowrate is less than 2 l/min [**8**].

Besides grinding force and material removal rate, the grinding ratio (G-ratio), which is related to cost and productivity, is also a major factor in heavy-duty grinding. Hence, a proper method is required for the selection of grinding parameters to ensure grinding efficiency and quality. An optimal grinding result should balance the major grinding output parameters such as grinding force, materials removal rate, and G-ratio.

Orthogonal experimental design is often used for optimizing production and process conditions. Orthogonal tolerance design, in a narrow sense, can be regarded as identical to parameter design, but in a broad sense, it is a subset of robust design, where the signal-to-noise ratio (SNR) is a major tool used in robust design [**9**]. The SNR can be used to replace the average value and to convert the trial results into a value for the evaluation of characteristics in an optimization analysis as it can reflect both the average and the variation of quality characteristics, i.e. it can estimate the variability in product quality [**10**].

In this paper, a set of empirical models of grinding force is built up based on orthogonal experimental data and these models have been verified through further experiments. Subsequently, a new performance index, which includes the specific material removal rate, size accuracy, wheel wear, and grinding forces, is proposed to evaluate the effect of heavy-duty grinding. Two major tools in robust design, (a) orthogonal arrays that accommodate many parameters, and (b) the SNR that measures quality with emphasis on variation, are tightly integrated in order to estimate the consistency of experiment design and optimal grinding parameters.

2 EXPERIMENTAL CONDITIONS AND METHODOLOGY

The aim of the experimental research attempts to find those optimal or compromise grinding strategies for better grinding performance under low cost constraint with different groups of grinding parameters. In order to assess the performance of heavy-duty grinding, an offline inspection was undertaken to measure G-ratio and size error. All of the experiments were carried out on a five-axis CNC machine centre. Coolant was delivered under 5 MPa pressure to the exit of the nozzle. The coolant used was a 9 per cent emulsion (Hocut 3380). The grinding power was recorded directly from the CNC controller and the grinding forces were monitored using a three-component force dynamometer 9272A. A data acquisition system was set up based on the LabView platform (NI-PCI6071E data logging card + self-developed software). The detailed experiment conditions are listed in Table 1.

The grinding experiment and analysis procedure is illustrated in Fig. 1. It consists of the following steps by:

(a) selecting grinding parameters;
(b) planning orthogonal design and SNR design;

Table 1 Experimental conditions

Machine tools	Five-axis CNC machine centre (spindle max. power 18.5 kW)
Workpiece	HP NGV blade made of CMSX4(HRC52)
Wheel	Al_2O_3 wheels (XA60E13VRP)
Coolant fluid	Hocut 3380, diluted rate 9%, pressure at 70 bar (the nozzle at 50 bar)
Depth of cut	$a_e = 0.5$–2.5 mm
Grinding width	$b = 9.5$–18 mm
Workspeed	$v_w = 500$–2000 mm/min
Wheel speed	$v_c = 30$–55 m/s
Grinding direction	Surface downgrinding, surface upgrinding

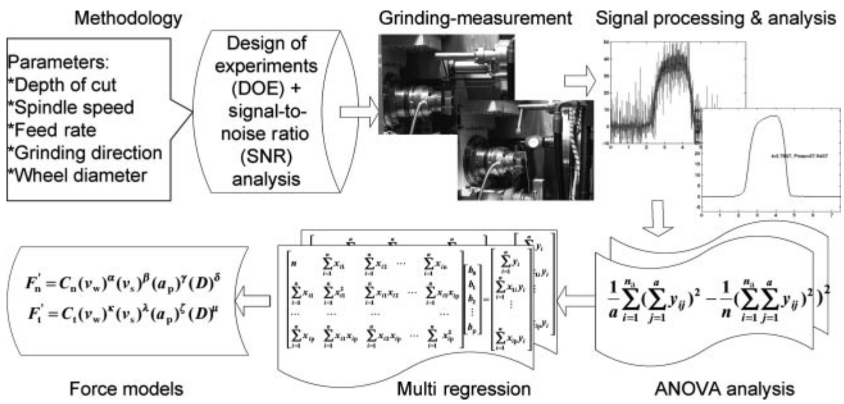

Fig. 1 Grinding experiment and analysis procedure

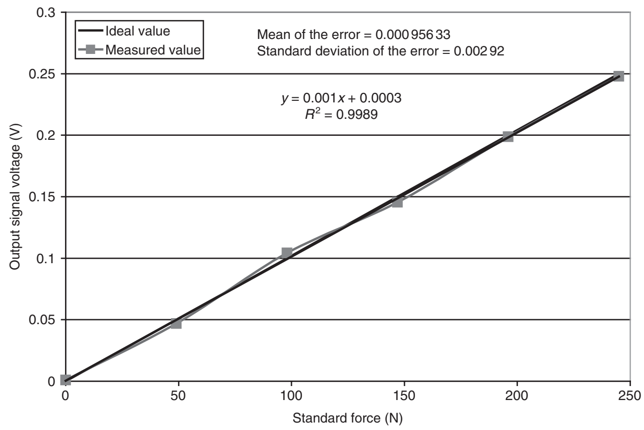

Fig. 2 Calibration of dynamometer and amplifier (F_x = normal force)

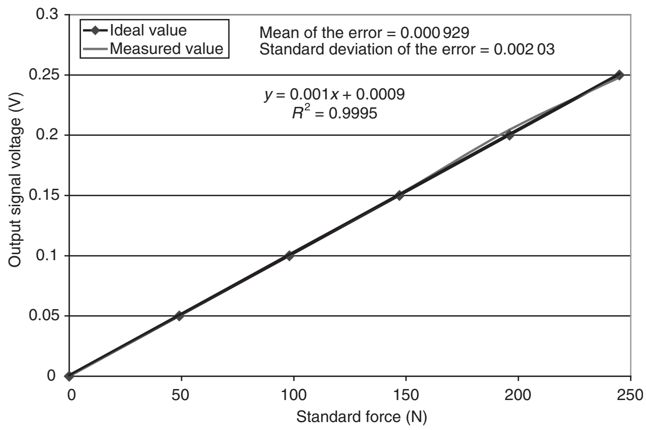

Fig. 3 Calibration of dynamometer and amplifier (F_y = tangential force)

(c) monitoring the progress of experiments and obtaining experimental data;
(d) filtering and analysing experimental data;
(e) finding the best experimental conditions and predicting latent experimental results by statistic analysis;
(f) building the empirical models based on multiple regression.

The experiments need to investigate the influence of exact depth of cut and real wheel diameter, which were measured after each cut. The G-ratio and size error can be obtained accordingly. Before experiments were undertaken, the dynamometer 9272A was carefully calibrated as shown in Figs 2 and 3.

3 GRINDING FORCE MODELLING

As is well known, theoretical models are too complex because the physical interrelationships must be defined accurately. Empirical models usually give good correlation for the range in which the equations were determined if all the important variables have been taken into consideration. Empirical models are, however, limited to specific situations because some parameters are uncontrollable in the grinding process. An empirical model is established by means of the values measured that have been obtained in grinding tests; that is, the model parameters are determined with the aid of regression analysis methods on the basis of numerous measured values. According to the application requirement, grinding tests are carried out to identify the relationship between all input and output quantities of interests. Then, the coefficients are determined and the empirical model can be verified for further use.

As already mentioned, empirical models can be built up by using the analysis of regression and variance to process the data from multifactor orthogonal experiments about the parameters v_c, v_w, a_e, and d_e. Because of different test conditions, the parameters of empirical models might be different. However, empirical formulas in grinding relate grinding forces (F_n or F_t) to workpiece speed (v_w), wheel speed (v_c), and depth of cut (a_e), which can also be verified individual experiments

$$\begin{aligned} F_n' &= C_n(v_w)^{\alpha}(v_c)^{\beta}(a_e)^{\gamma}(d_e)^{\delta} \\ F_t' &= C_t(v_w)^{\kappa}(v_c)^{\lambda}(a_e)^{\zeta}(d_e)^{\rho} \end{aligned} \tag{1}$$

where α, β, γ, δ, κ, λ, ζ, and ρ are the parameters that need to be computed through experiments.

A complex non-linear problem can be regarded as an extension of the usual linear model in a sense. These non-linear problems can still be converted to linear form via a suitable transformation. Equation (1) can be linearized by taking logarithms as follows

$$\begin{aligned}\log(F_n') &= \log(C_n) + \alpha\log(v_w) + \beta\log(v_c) \\ &\quad + \gamma\log(a_e) + \delta\log(d_e) \\ \log(F_t') &= \log(C_t) + \kappa\log(v_w) + \lambda\log(v_c) \\ &\quad + \zeta\log(a_e) + \rho\log(d_e)\end{aligned} \tag{2}$$

which is linear in the parameters $\log(C_n)$, α, β, γ, or $\log(C_t)$, κ, λ, ζ. Note, however, that it is not linear in the original parameters $\log(C_n)$, α, β, γ, or $\log(C_t)$, κ, λ, ζ. This is clearly seen by examining the error term. If the transformed error term is to have zero expectation with variance σ^2, then the error variable in the original models must have a more complex distributional form [**11**].

In grinding, if there are p factors that can influence grinding forces, the observations will be: y_i, x_{i1}, x_{i2}, x_{i3}, ..., x_{ip} ($i = 1, 2, \ldots, n$), n being the number of the experiments. If the relationship of response variable y_i and independent variable x_{in} is linear, a multiple linear regression method can be used to build up a multifactor empirical model. A regression model can be set as follows [**11**]

$$y = \beta_0 + \beta_1 x_1 + \beta_2 x_2 + \beta_3 x_3 + \cdots + \beta_p x_p + \varepsilon \tag{3}$$

where β_p stands for regression coefficients and ε is the error.

Let b be trial values for β. The regression equation will be

$$\hat{y} = b_0 + b_1 x_1 + b_2 x_2 + b_3 x_3 + \cdots + b_p x_p \tag{4}$$

Generally, the difference $\varepsilon = y_i - \hat{y}$, which is called a residual, will not be zero because the response fluctuates around the expected value. The method of least squares selects b to minimize the sum of squared differences; the normal equation is presented as follows

$$\begin{bmatrix} n & \sum_{i=1}^n x_{i1} & \sum_{i=1}^n x_{i2} & \cdots & \sum_{i=1}^n x_{in} \\ \sum_{i=1}^n x_{i1} & \sum_{i=1}^n x_{i1}^2 & \sum_{i=1}^n x_{i1}x_{i2} & \cdots & \sum_{i=1}^n x_{i1}x_{ip} \\ \cdots & \cdots & \cdots & \cdots & \cdots \\ \sum_{i=1}^n x_{ip} & \sum_{i=1}^n x_{i1}x_{ip} & \sum_{i=1}^n x_{i2}x_{ip} & \cdots & \sum_{i=1}^n x_{ip}^2 \end{bmatrix} \begin{bmatrix} b_0 \\ b_1 \\ b_2 \\ \vdots \\ b_p \end{bmatrix} = \begin{bmatrix} \sum_{i=1}^n y_i \\ \sum_{i=1}^n x_{1i} y_i \\ \vdots \\ \sum_{i=1}^n x_{ip} y_i \end{bmatrix} \tag{5}$$

In practical use, the regression equation is often presented as

$$y_i = \mu_0 + \beta_1(x_{i1} - x_1) + \beta_2(x_{i2} - x_2) + \cdots + \beta_p(x_{ip} - x_p) + \varepsilon_i \quad i = 1, 2, \ldots, n \tag{6}$$

where $x_i = 1/n\sum_{k=1}^n x_{ki}$, $i = 1, 2, \ldots, n$, apparently, $\mu_0 - \sum_{k=1}^n \beta_i x_i = b_i$.

Setting $l_{ij} = \sum_{k=1}^n x_{ki}x_{kj} - n\bar{x}_i\bar{x}_j$, $i, j = 1, 2, \ldots, p$, $l_{jy} = \sum_{i=1}^n x_{ij} y_i - n\bar{x}_i y$, $j = 1, 2, \ldots, p$. Hence, the normal equations can be transformed as

$$\boldsymbol{Ab} = \boldsymbol{B} \quad \text{or} \quad \boldsymbol{b} = \boldsymbol{A}^{-1}\boldsymbol{B} \tag{7}$$

where $\boldsymbol{A}$ is the coefficient matrix of the normal equation

$$\mathbf{A} = \begin{bmatrix} n & 0 \\ 0 & L \end{bmatrix}, \mathbf{B} = \begin{bmatrix} \sum_{i=1}^n y_i \\ l_{1y} \\ l_{2y} \\ \vdots \\ l_{py} \end{bmatrix}, \mathrm{L} = \begin{bmatrix} l_{11} & l_{12} & \cdots & l_{1p} \\ l_{21} & l_{22} & \cdots & l_{2p} \\ \cdots & \cdots & \cdots & \cdots \\ l_{p1} & l_{p2} & \cdots & l_{pp} \end{bmatrix}$$

$$\boldsymbol{b} = \begin{bmatrix} \mu_0 \\ b_1 \\ b_2 \\ \vdots \\ b_p \end{bmatrix} = \begin{bmatrix} 1/n & 0 \\ 0 & L^{-1} \end{bmatrix} \begin{bmatrix} \sum_{i=1}^n y_i \\ l_{1y} \\ l_{2y} \\ \vdots \\ l_{py} \end{bmatrix}$$

Hence, $\mu_0 = 1/n\sum_{i=1}^n y_i = y$. The coefficients of a regression equation can be presented as

$$\begin{cases} b_0 = \bar{y} - \sum_{i=1}^p b_i x_i \\ \begin{bmatrix} b_1 \\ b_2 \\ \vdots \\ b_p \end{bmatrix} = L^{-1} \begin{bmatrix} l_{1y} \\ l_{2y} \\ \vdots \\ l_{py} \end{bmatrix} \end{cases} \tag{8}$$

The quality of a regression equation can be measured by the coefficient of determination R^2: ($R = +\sqrt{R^2}$ is called the multiple correlation coefficient). Setting $SS_\mathrm{R} = \sum_{i=1}^n(\hat{y}_i - y)^2$, $SS_\mathrm{E} = \sum_{i=1}^n(y_i - \hat{y}_i)^2$, $SS_\mathrm{T} = \sum_{i=1}^n(y_i - y)^2 = \sum_{i=1}^n y_i^2 - 1/n\left(\sum_{i=1}^n y_i\right)^2$, there is

$$R^2 = \frac{SS_\mathrm{E}}{SS_\mathrm{T}} \quad \text{or} \quad R = \sqrt{\frac{SS_\mathrm{E}}{SS_\mathrm{T}}} \tag{9}$$

Here R equals 1 if the fitted equation passes through all the data points, so error $\varepsilon_\mathrm{i} = 0$ for all i. At the other extreme, if R is 0, the predictor variables x_1, x_2, ..., x_p have no influence on the response. Another method in assessing the effects of particular predictor variables is the likelihood ratio test for the regression coefficients (F-test). In fact, the coefficient of determination R^2 has a close relationship with F. The larger the R^2, the larger the F as well.

Considering that the force in upgrinding is different from that in downgrinding, it is more rational to build up empirical models separately. Tables 2 and 3 show the data for the two separate orthogonal experiments. In Tables 2 and 3, factor A is feed rate; its level 1 is 8.3 mm/s, level 2 is 16.67 mm/s, level 3 is 25 mm/s, and level 4 is 33.33 mm/s. Factor B is the spindle speed; its level 1 is 30 m/s, level 2 is 35 m/s, level 3 is 40 m/s, and level 4 is 45 m/s. Factor C is the depth of cut; its level 1 is 0.5 mm, level 2 is 1 mm, level 3 is 1.5 mm, and level 4 is 2 mm. Factor D is the grinding wheel diameter; its level 1 is 110 mm, and level 2 is 140 mm. Based on equations (6) to (9) and experimental data in Tables 2 and 3, the empirical force models can be regressed as equation (10).

Table 2 Downgrinding force data, $L_{16}(4^5)$

Number	v_w (mm/s)	v_c (m/s)	a_e (mm)	d_e (mm)	F_n (N/mm)	F_t (N/mm)
1	8.33	30	0.493	126.4	24.048	10.133
2	8.33	35	0.941	121.9	36.051	14.015
3	8.33	40	1.435	129.7	45.794	17.341
4	8.33	45	1.891	134.9	70.34	23.783
5	16.67	30	0.932	127.5	40.424	18.413
6	16.67	35	0.475	138.0	24.071	12.125
7	16.67	40	1.913	113.6	98.64	34.244
8	16.67	45	1.418	119.6	72.461	27.889
9	25	30	1.433	136.0	87.54	32.526
10	25	35	1.843	128.6	95.121	36.244
11	25	40	0.473	126.4	29.761	11.756
12	25	45	0.934	136.0	49.671	20.527
13	33.33	30	1.762	119.6	108.69	39.433
14	33.33	35	1.321	114.8	78.978	33.16
15	33.33	40	0.913	133.9	68.787	23.857
16	33.33	45	0.438	130.7	31.756	14.788

Table 3 Upgrinding force data, L_{16} (4^5)

Number	v_w (mm/s)	v_c (m/s)	a_e (mm)	d_e (mm)	F_n (N/mm)	F_t (N/mm)
1	8.33	30	0.487	127.5	24.496	10.575
2	8.33	35	0.939	120.7	38.041	7.681
3	8.33	40	1.425	131.8	45.727	8.769
4	8.33	45	1.901	134.9	64.573	8.211
5	16.67	30	0.93	132.9	42.068	11.814
6	16.67	35	0.481	137.0	25.752	9.551
7	16.67	40	1.853	112.4	89.959	10.982
8	16.67	45	1.441	118.4	62.312	7.872
9	25	30	1.373	136	68.268	11.244
10	25	35	1.799	131.8	93.52	11.956
11	25	40	0.457	125.3	25.697	8.188
12	25	45	0.927	134.9	49.292	9.016
13	33.33	30	1.757	130.7	102.19	13.133
14	33.33	35	1.237	112.4	88.524	12.135
15	33.33	40	0.903	137	62.112	10.565
16	33.33	45	0.457	123.0	32.053	10.021

$$\begin{aligned} F'_{\mathrm{n\,UP}} &= 13\,260(v_w)^{0.352}(v_c)^{-0.204}(a_e)^{0.827}(d_e)^{-0.706} \\ F'_{\mathrm{t\,UP}} &= 630.59(v_w)^{0.177}(v_c)^{-0.694}(a_e)^{0.082}(d_e)^{-0.193} \\ F'_{\mathrm{n\,DOWN}} &= 795.6(v_w)^{0.380}(v_c)^{-0.004}(a_e)^{0.875}(d_e)^{-0.253} \\ F'_{\mathrm{t\,DOWN}} &= 533.44(v_w)^{0.393}(v_c)^{-0.121}(a_e)^{0.724}(d_e)^{-0.256} \end{aligned} \tag{10}$$

Figure 4(a) presents the residual case order plot of the specific normal force in down grinding. The plot shows the residuals plotted in case order. The 99 per cent confidence intervals about these residuals are plotted as error bars. The first observation of F_n is an outlier since its error bar does not cross the zero reference line, which means this observed value deviates from the regression equation. The R^2 of the regression equation is about 0.967, indicating the model accounts for over 97 per cent of the variability in the observations. The F-test value (for the hypothesis test that all the regression coefficients are zero) is 81.54. Figure 4(b) demonstrates the residual case order plot of the specific tangential force in downgrinding. The 11th observation of F_t is deviated from the regression equation. The determination coefficient R^2 of the regression equation is about 0.976 and the F-test value is 113.6.

Figure 5(a) is the residual case order plot of the specific normal force in upgrinding. The R^2 of the regression equation is about 0.971, indicating the model accounts for over 98 per cent of the variability in the observations. The F-test value is 93.17. Figure 5(b) is the residual case order plot of the specific tangential force in upgrinding. The correlation coefficient R^2 of the regression equation is about 0.873 and the F-test value is 8.38. According to the degree of

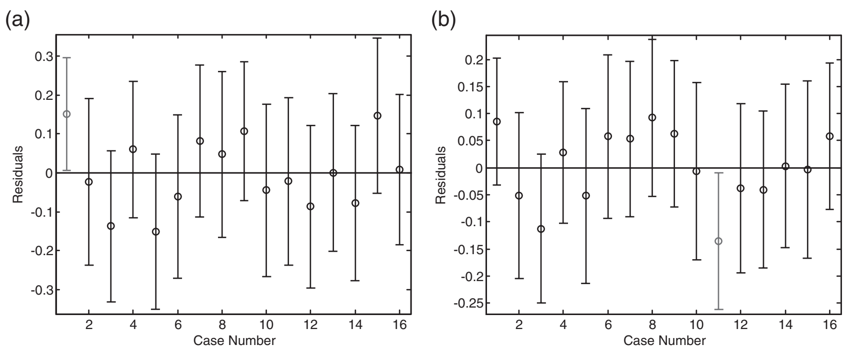

Fig. 4 Residual case order plot in downgrinding; (a) specific normal force (F_n); (b) specific tangential force (F_t)

freedom (p, $n-p-1$) and percentage points $F_{(p,n-p-1)}$ of the F-distribution, $F_{(4,11)}$ is 5.67. Apparently, it is highly unlikely that all the coefficients are zero, and all the regression equations are completely acceptable. For the specific tangential force model of upgrinding, the correlation coefficient R and F-test value are lower than the others. This is because the difference of the specific tangential force in upgrinding is quite small, so that variation of grinding parameters cannot clearly be reflected.

The effects of the empirical models must be verified through a set of trials. After modelling, a set of new experiments was conducted. Figure 6(a) compares the modelled values with the measured values of the specific normal force in downgrinding. The correlation coefficient R is 0.98. The mean of the error is 0.73 N/mm, and the range of the error is 5.60. Figure 6(b) compares the specific tangential force of the values modelled with the values measured in downgrinding. The correlation coefficient R is 0.98. The mean of the error is 0.26 N/mm, and the range of the error is 1.77 N/mm. Figure 7(a) compares the specific normal force of the values modelled with the values measured in upgrinding. The correlation coefficient R is 0.98. The mean of the error is 0.18 N/mm, and the range of the error is 4.93 N/mm. Figure 7(b) compares the specific tangential force of the values modelled with values

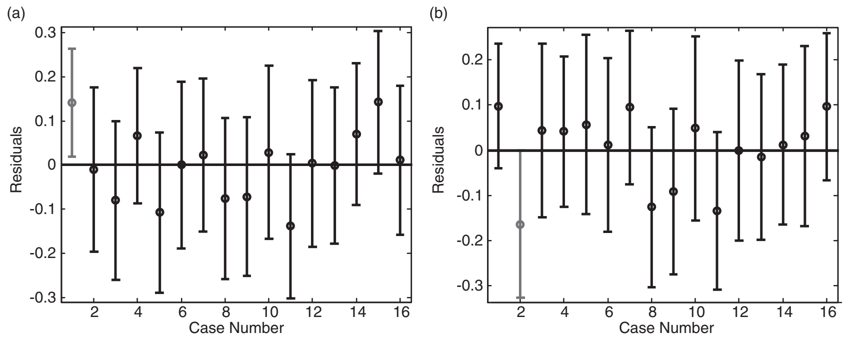

Fig. 5 Residual case order plot in upgrinding; (a) specific normal force; (b) specific tangential force

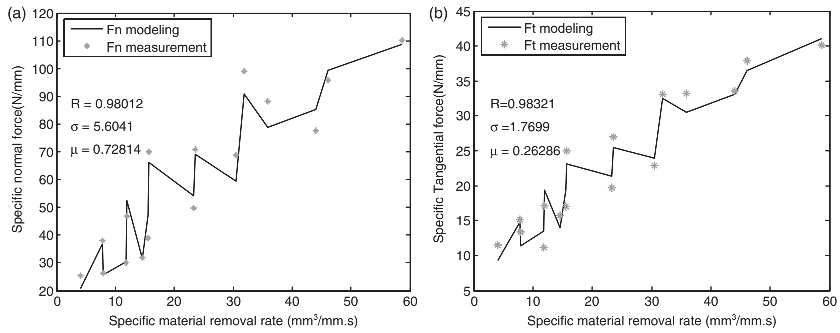

Fig. 6 Force modelled values and verified trial values in downgrinding; (a) specific normal force F_n; (b) specific tangential force F_t

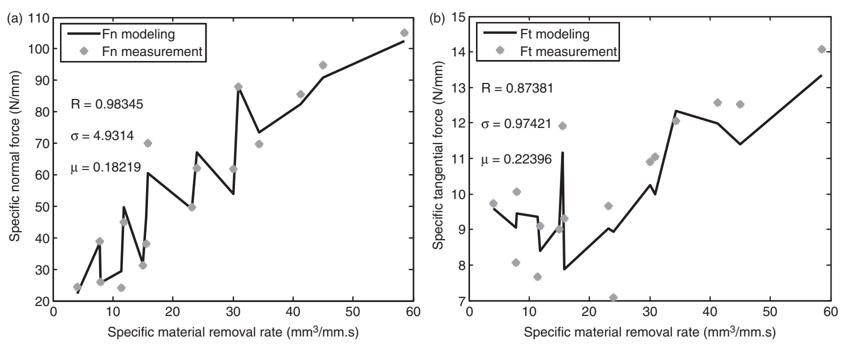

Fig. 7 Upgrinding force modelled values and verified trial values; (a) specific normal force F_n; (b) specific tangential force F_t

measured in upgrinding. The correlation coefficient R is 0.87. The mean of the error is 0.22 N/mm, and the range of the error is 0.97 N/mm. This demonstrates that the predicted model data match the experimental data for real grinding operations with over 95 per cent correlation.

4 DESIGNS AND ANALYSIS OF ROBUST EXPERIMENTS

Based on an analysis of the grinding process, a set of grinding parameters was proposed for investigation. In fact, the grinding process, to a vast extent, is a process of interactions among wheels, workpiece materials, and coolant. Besides the characteristics and the technical behaviour of the grinding wheels themselves, the workpiece material to be ground is of fundamental importance. The behaviour of the material is characterized by its physical properties and the different material removal rate depends on the ductility (elongation) [**12**].

To evaluate grinding performance, it is necessary to apply orthogonal experiments. A large depth of cut will result spontaneously in a high grinding force, so force alone cannot be used for assessing which grinding condition is the most appropriate. In heavy-duty grinding, besides grinding forces, the specific material removal rate Q_{w}', size accuracy, and G-ratio also reflect grinding quality. Considering that a good heavy-duty grinding should give a large specific material removal rate, a high G-ratio, small grinding forces, and a small size error, a new evaluated index is introduced based on these influencing factors as follows

$$\varpi = \frac{Q_{\mathrm{w}}'}{F_{\mathrm{r}}'} \frac{G}{a_{\mathrm{e}}/a_{\mathrm{e}}'} \tag{11}$$

where a_{e}' is the real depth of cut and F_{r}' is the consultant grinding force. The larger the index, the better the grinding performance is.

In order comprehensively to assess the effects of the parameters selected, orthogonal experimental design is often used for statistic analyses of performance. Orthogonal experimental design could utilize partial experiments rather than full experiments to predict the influence of each experimental factor and calculate the dependency of the results on the experimental factors. The dependency values of orthogonal experimental design are the percentage contributions based on the analysis of variance. Even under the same conditions, each test is unable to repeat the same results exactly, owing to experimental random errors. The fluctuation of the result can be regarded as a kind of noise interference. The SNR method of experiments consolidates several repetitions into one value that reflects the amount of variation present. Combining SNR with orthogonal experiments, different experiment characteristics under partial experimental conditions can be valued and predicted appropriately.

Let $\bar{Y} = (Y_1, Y_2, \ldots, Y_{n_{\mathrm{r}}})$ be a distribution of observations that includes noise interference. The quality of an experiment can be described by the SNR [**13**]

$$\eta = 10 \log\left[\frac{1}{n_{\mathrm{r}}}(S_{n_{\mathrm{r}}} - S_{n_{\mathrm{r}}}^{*})/S_{n_{\mathrm{r}}}^{*}\right] \tag{12}$$

where $S_{n_{\mathrm{r}}} = 1/n_{\mathrm{r}}\left(\sum_{i=1}^{n_{\mathrm{r}}} Y_i\right)^2$, $S_{n_{\mathrm{r}}}^{*} = 1/(n_{\mathrm{r}}-1)\left(\sum_{i=1}^{n_{\mathrm{r}}} Y_i - \bar{Y}\right)^2$; n_{r} is the number of repetitions of observations. In equation (12), $S_{n_{\mathrm{r}}}^{*}$ reflects the fluctuation of the experimental error and $(S_n - S_n^{*})/n_{\mathrm{r}}$ represents the pure effect of a signal after eliminating errors; $[1/n_{\mathrm{r}}(S_{n_{\mathrm{r}}} - S_{n_{\mathrm{r}}}^{*})/S_{n_{\mathrm{r}}}^{*}]$ is the mean-square deviation for the output characteristic. Simply speaking, η is the ratio of mean (signal) to standard deviation (noise). It is a logarithmic function based on the mean-square deviation around the target.

When the performance characteristic Y is measured on a continuous scale, it usually takes one of three forms:

(a) smaller the better (STB);
(b) larger the better (LTB); or
(c) nominal (specific target value) the best (NTB).

For example, roughness of grinding requires STB and G-ratios need LTB. In terms of equation (12), a better result is represented by a higher evaluated index. Therefore, the SNR η will be

$$\eta = 10 \log \frac{1}{\frac{1}{n_{\mathrm{r}}}\sum_{i=1}^{n_{\mathrm{r}}} \frac{1}{Y_i^2}} = -10 \log\left(\frac{1}{n_{\mathrm{r}}} \sum_{i=1}^{n_{\mathrm{r}}} \frac{1}{Y_i^2}\right) \tag{13}$$

Clearly, for roughness, smaller roughness means a larger η; also, a larger evaluated index implies a larger η. Table 4 shows the experimental data of heavy-duty grinding by Al_2O_3 wheels for the evaluated index ϖ_n. In each group, wheel speed, workpiece feed rate, depth of cut, and wheel diameter were chosen as independent variables (i.e. influential factors). Each independent variable has four levels, whereas grinding direction and grinding wheel diameter were selected as having two levels. Therefore, a blend orthogonal array of $L_{16}(4^3 \times 2^6)$ is appropriate in this case for all the SNR experiments. If, however, full factor experiments were adopted, the number of a blend experiment would be 68 runs. When the orthogonal array of $L_{16}(4^3 \times 2^6)$ is selected, only 16 runs would be carried out. Clearly, the saving in both money and time are significant.

In Table 4, parameter A is feed rate; its level 1 is 8.3 mm/s, level 2 is 16.67 mm/s, level 3 is 25 mm/s, and level 4 is 33.33 mm/s. Parameter B is the spindle speed; level 1 is 30 m/s, level 2 is 35 m/s, level 3 is 40 m/s, and level 4 is 45 m/s. Parameter C is the depth of cut; level 1 is 0.5 mm, level 2 is 1 mm, level 3 is

Table 4 Experimental data of heavy-duty grinding [$L_{16}(4^3 \times 2^6)$]

Trial number	A v_w	B v_c	C a_e	D d_e	E direction	F	G	H	I	Evaluated index and SNR ϖ_1	ϖ_2	ϖ_3	η
1	1 (8.33)	1 (30)	1 (0.5)	1 (110)	1 (up)	1	1	1	1	303.37	305.12	301.42	49.64
2	1 (8.33)	2 (35)	2 (1)	1 (110)	1 (up)	2	2	2	2	366.99	381.67	363.35	51.37
3	1 (8.33)	3 (40)	3 (1.5)	2 (140)	2 (down)	1	1	2	2	452.17	470.26	447.69	53.19
4	1 (8.33)	4 (45)	4 (2)	2 (140)	2 (down)	2	2	1	1	296.55	308.41	293.61	49.52
5	2 (16.77)	1 (30)	2 (1)	2 (140)	2 (down)	1	2	1	2	544.36	540.75	538.97	54.67
6	2 (16.77)	2 (35)	1 (0.5)	2 (140)	2 (down)	2	1	2	1	549.90	550.24	544.46	54.78
7	2 (16.77)	3 (40)	4 (2)	1 (110)	1 (up)	1	2	2	1	569.35	568.17	570.13	55.11
8	2 (16.77)	4 (45)	3 (1.5)	1 (110)	1 (up)	2	1	1	2	559.10	581.47	553.57	55.03
9	3 (25)	1 (30)	3 (1.5)	1 (110)	2 (down)	2	2	2	1	547.35	569.24	541.93	54.85
10	3 (25)	2 (35)	4 (2)	1 (110)	2 (down)	1	1	1	2	566.88	565.87	561.26	55.04
11	3 (25)	3 (40)	1 (0.5)	2 (140)	1 (up)	2	2	1	2	532.34	553.64	527.07	54.60
12	3 (25)	4 (45)	2 (1)	2 (140)	1 (up)	1	1	2	1	523.00	543.92	517.82	54.45
13	4 (33.33)	1 (30)	4 (2)	2 (140)	1 (up)	2	1	2	2	563.90	562.11	558.32	54.99
14	4 (33.33)	2 (35)	3 (1.5)	2 (140)	1 (up)	1	2	1	1	476.31	474.89	471.59	53.52
15	4 (33.33)	3 (40)	2 (1)	1 (110)	2 (down)	2	1	1	1	488.76	489.87	483.92	53.76
16	4 (33.33)	4 (45)	1 (0.5)	1 (110)	2 (down)	1	2	2	2	487.32	506.82	497.48	53.93
I_j	203.72	214.14	212.95	428.72	428.71	429.53	430.87	425.78	425.62				$\Sigma\eta_i = 858.435$
II_j	219.58	214.71	214.25	429.72	429.73	428.90	427.57	432.66	432.81				$(\Sigma\eta_i)^2/n = 46\,056.94$
III_j	218.94	216.66	216.58										$S_E = 6.892$
IV_j	216.19	212.93	214.65										$\Sigma\eta_i^2 = 46\,108.61$
ω_{j1}	50.93	53.53	53.24	53.59	53.59	53.69	53.86	53.86	53.20				$\mu = (\Sigma\eta_i)/n = 53.652$
ω_{j2}	54.90	53.68	53.56	53.71	53.72	53.61	53.45	53.45	54.10				$SS_T = 51.663$
ω_{j3}	54.73	54.16	54.15	0.00	0.00	0.00	0.00	0.00	0.00				$\Sigma S_R = 44.77$
ω_{j4}	54.05	53.23	53.66										
Range	3.97	0.93	0.91	0.13	0.13	0.08	0.41	0.41	0.90				
Q_A	46 098.08	46 058.75	46 058.64	46 057.01	46 057.01	46 056.97	46 057.62	46 059.90	46 060.18				
SS_R	41.14	1.81	1.70	0.06	0.06	0.02	0.68	2.95	3.23				

Table 5 Table for sources of variance

Source	Sum of squares (SS_{Rj})	Degree of freedom	Mean square (SS_{Rj}/f_j)	F-ratio	$F_{1-\alpha}(f_j f_e)$ (standard)
A(v_w)	41.14	3	13.71	7.96	4.19 (0.1)
B(v_c)	1.81	3	0.60	0.35	6.59 (0.05)
C(a_e)	1.70	3	0.57	0.33	
D(d_e)	0.06	1	0.06	0.04	
E (up/down)	0.06	1	0.06	0.04	
Error	6.89	4	1.72		

1.5 mm, and level 4 is 2 mm. Parameter D is the grinding wheel diameter; level 1 is 110 mm, and level 2 is 140 mm. Parameter E is the grinding direction; level 1 is upgrinding, and level 2 is downgrinding. Define ω_{j1} as an unbiased estimator under j factor of level 1 ($\omega_{j1} = (\mathrm{I}_i/n_a) - \mu$); ω_{j2} is an unbiased estimator under j factor of level 2 ($\omega_{j2} = (\mathrm{II}_i/n_a) - \mu$); ω_{j3} is an unbiased estimator under j factor of level 3 ($\omega_{j3} = (\mathrm{III}_i/n_a) - \mu$); ω_{j4} is an unbiased estimator under j factor of level 4 ($\omega_{j4} = (\mathrm{IV}_i/n_a) - \mu$), where μ is mean and n_a is the level number within a factor. These unbiased estimators can play important roles in predicting a group of optimum parameters. Each measurement of the force and size accuracy was repeated three times. The evaluated index values were calculated and shown in Table 4. Table 5 indicates the sources of variance.

From Table 4, the maximum SNR value is η_7 and the corresponding parameters are $A_2B_3C_4D_1E_1$, i.e. $v_w = 16.67$ mm/s, $v_c = 40$ m/s, $a_e = 2$ mm, $d_e = 110$ mm, and upgrinding. Moreover, SNR η_i can be further analysed by using ANOVA. As can be seen in Table 5, factor A (feed rate) is significant in a 95 per cent confidence interval, which means that it can influence the evaluated index to a great extent. This is because the increment change of feed rate is larger than other parameters, such as depth of cut and size accuracy, for the specific material removal rate.

One of the benefits of orthogonal design is that it can predict a better set of parameters from existing experimental outcomes. Taking the maximum values from the unbiased estimates in each factor column, for example, ω_{12}, ω_{23}, ω_{33}, ω_{42}, ω_{52} in Table 4, its average estimated value $\hat{Y} = \omega_{12} + \omega_{23} + \omega_{33} + \omega_{42} + \omega_{51} - 4\mu = 55.32$ (dB). The confidence interval of $\hat{Y}$ is $(\hat{Y} - \delta,\ \hat{Y} + \delta)$ and δ can be calculated as follows [**14**]

$$\delta = \sqrt{\frac{F_\alpha(1, \tilde{f}_e)SS_E}{n_e\tilde{f}_e}} \tag{14}$$

where $\tilde{f}_e + f_e + \Sigma$ (degree of freedom of insignificant factors); $SS_E = S_E + \Sigma$ (sum of squares for insignificant factors); n_e = total trial number/[$1 + \Sigma$ (degree of freedom of significant factors]; $F_\alpha(1, \tilde{f}_e)$ can be obtained through F-test tables ($F_{(1,12)} = 4.75$). In this case, $\delta = 1.02$, so the confidence interval of $\hat{Y}$ is (54.30, 56.34).

Table 6 Verified trials under a better condition

Number	a_e	d_e	F_n	F_t	F_r	Q'_w	ϖ
1	1.418	135.964	61.472	22.515	65.4655	23.633	535.79
2	1.432	133.896	63.034	25.263	67.908	23.867	526.77
3	1.452	129.644	65.147	26.132	70.193	24.200	533.97
4	1.429	112.394	60.254	23.343	64.618	23.817	561.81
5	1.435	127.496	62.711	24.621	67.371	23.917	543.39

In other words, when $v_w = 16.67$ mm/s, $v_c = 40$ m/s, $a_e = 1.5$ mm, $d_e = 140$ mm, and downgrinding ($A_2B_3C_3D_2E_2$), the range of the evaluated index will be from 54.30 to 56.34.

In terms of the better conditions of $A_2B_3C_3D_2E_2$, verification tests were carried out five times. Table 6 demonstrates the results of the trials. The SNR can be calculated as

$$\begin{aligned}\eta &= -10\log[(1/535.79^2 + 1/526.77^2 + 1/533.97^2 \\ &\quad + 1/561.81^2 + 1/543.39^2)/5] \\ &= 54.65\end{aligned}$$

Clearly, the estimated range is the right location. Further, it was noticed that the error of estimation would be smaller when using SNR compared with using average index values [**9**]. In this case, the result of SNR is four times better than that of the average values.

5 CONCLUSIONS

By means of orthogonal experiments, the empirical models of a grinding force can be established statistically. Grinding performance, assessed by a multiple regression methodology, can be presented and evaluated by correlation coefficients, error residuals, and F-statistics. F-distribution analysis displays that multiple regression equations are acceptable. Through verification experiments, the predicted data from empirical models agrees well with the data measured in grinding trials. The correlation coefficients of the empirical models and real measurement are between 0.86 and 0.97. These force models can provide a concrete foundation for the design of grinding fixtures. Also, while selecting appropriate grinding parameters, orthogonal experiment design based on SNR is a better approach for completely randomized experiments. The results, based on the analysis of variance and optimization, can provide very useful and reliable information. Aiming for maximum specific material removal rate, minimum grinding force, best size accuracy, and largest G-ratio, a new performance index was introduced for assessing the heavy-duty grinding of nickel-based alloy CMSX4. By means of robust experimental design, a better grinding performance under a set of grinding parameters can be predicted and the influence range of the evaluated index can be estimated rationally according to their confidence intervals. Optimal grinding conditions are found for the achievement of the desired maximum specific material removal rate with the minimum specific grinding force.

ACKNOWLEDGEMENTS

The authors wish to acknowledge the support of Rolls-Royce plc.

REFERENCES

1 **Hitchiner, M.** Grinding of aerospace alloys with vitrified CBN. *Abrasives*, December 1998/January 1999, 25–32.
2 **Tönshoff, H. K., Friemuth, T.,** and **Becker, J. C.** Process monitoring in grinding. *CIRP Ann., Mfg Technol.*, 2002, **51**(2), 551–571.
3 **Stephenson, D. J., Jin, T.,** and **Corbett, J.** High efficiency deep grinding of a low alloy steel with plated CBN wheels. *Ann. CIRP*, 2002, **51**(1), 241–244.
4 **Tönshoff, H. K., Wobker, H.-G.,** and **Brunner, G.** CBN grinding with small wheels. *Ann. CIRP*, 1995, **44**(1), 311–316.
5 **Malkin, S.** Grinding technology theory and applications of machining with abrasives, 1994 (Ellis Horwood Ltd, Chichester, UK).
6 **Tönshoff, H. K.** Modelling and simulation of grinding processes. *Ann. CIRP*, 1992, **41**(2), 677–688.
7 **Chen, X.** and **Rowe, W. B.** Modelling surface roughness improvement in grinding. *Proc. Instn Mech. Engrs, Part B: J. Engineering Manufacture*, 1999, **213**(B1), 93–96.
8 **Brinksmeier, E., Heinzel, C.,** and **Wittmann, M.** Friction, cooling and lubrication in grinding. *CIRP Ann., Mfg Technol.*, 1999, **48**(2), 581–598.
9 **Park, S. H.** *Robust design and analysis for quality engineering*, 1996 (Chapman & Hall, London).
10 **Maghsoodloo, S.** and **Chang, C.-L.** Quadratic loss functions and signal-to-noise ratios for a bivariate response. *J. Mfg Systems*, 2001, **20**(1), 1–12.
11 **Hosmer, D. W.** and **Lemeshow, S.** 2nd edn. *Applied logistic regression*, 2000 (John Wiley & Sons, Canada).
12 **Kalpakjian, S.** and **Schmid, S. R.** Eds. *Manufacturing engineering and technology,* 4th edn, 2001 (Prentice-Hall International (UK) Ltd, London).
13 **Khoei, A. R., Masters, I.,** and **Gethin, D. T.** Design optimisation of aluminium recycling processes using Taguchi technique. *J. Mater. Processing Technol.*, 2002, **127**(1), 96–106.
14 **Montgomery, D., Montgomery, C.,** and **Runger, G. C.** 4th edn. *Applied statistics and probability for engineers,* 2006 (John Wiley & Sons, Hoboken, N.J.).